Second compartment widens plasmid invasion conditions: Two-compartment pair-formation model of conjugation in the gut

Jesse B. Alderliesten [a], Mark P. Zwart [b], J. Arjan G.M. de Visser [c], Arjan Stegeman [a], Egil A.J. Fischer [a,*]

[a] *Department of Population Health Sciences, Faculty of Veterinary Medicine, Utrecht University, Utrecht, the Netherlands*
[b] *Department of Microbial Ecology, The Netherlands Institute of Ecology (NIOO-KNAW), Wageningen, the Netherlands*
[c] *Laboratory of Genetics, Wageningen University & Research, Wageningen, the Netherlands*

A R T I C L E   I N F O

A B S T R A C T

Understanding under which conditions conjugative plasmids encoding antibiotic resistance can invade bacterial communities in the gut is of particular interest to combat the spread of antibiotic resistance within and between animals and humans. We extended a one-compartment model of conjugation to a two-compartment model, to analyse how differences in plasmid dynamics in the gut lumen and at the gut wall affect the invasion of plasmids. We compared scenarios with one and two compartments, different migration rates between the lumen and wall compartments, and different population dynamics. We focused on the effect of attachment and detachment rates on plasmid dynamics, explicitly describing pair formation followed by plasmid transfer in the pairs. The parameter space allowing plasmid invasion in the one-compartment model is affected by plasmid costs and intrinsic conjugation rates of the transconjugant, but not by these characteristics of the donor. The parameter space allowing plasmid invasion in the two-compartment model is affected by attachment and detachment rates in the lumen and wall compartment, and by the bacterial density at the wall. The one- and two-compartment models predict the same parameter space for plasmid invasion if the conditions in both compartments are equal to the conditions in the one-compartment model. In contrast, the addition of the wall compartment widens the parameter space allowing invasion compared with the one-compartment model, if the density at the wall is higher than in the lumen, or if the attachment rate at the wall is high and the detachment rate at the wall is low. We also compared the pair-formation models with bulk-conjugation models that describe conjugation by instantaneous transfer of the plasmid at contact between cells, without explicitly describing pair formation. Our results show that pair-formation and bulk-conjugation models predict the same parameter space for plasmid invasion. From our simulations, we conclude that conditions at the gut wall should be taken into account to describe plasmid dynamics in the gut and that transconjugant characteristics rather than donor characteristics should be used to parameterize the models.

© 2021 The Authors. Published by Elsevier Ltd. This is an open access article under the CC BY license (http://creativecommons.org/licenses/by/4.0/).

1. Introduction

Since the 1970s mathematical models have been used to determine under which conditions plasmids (extra-chromosomal DNA molecules) can invade and persist in populations of plasmid-free bacteria (Freter et al., 1983a; Simonsen, 1991; Stewart and Levin, 1977). Plasmids often carry antibiotic resistance genes, making the invasion of plasmids into new populations, such as the gut microbiota of animals and humans, of particular interest to combat the spread of antibiotic resistance within and between animals and humans (Dame-Korevaar et al., 2019; McInnes et al., 2020; Shintani et al., 2015; Shterzer and Mizrahi, 2015).

Plasmids can be transferred from a donor to a recipient bacterium in a process called conjugation (Smillie et al., 2010; Thomas and Nielsen, 2005). Plasmid genes can code for a variety of functions that are beneficial to the bacterial host, such as resistance against antibiotics and heavy metals, and the ability to use alternative metabolic pathways (Dib et al., 2015). Under other conditions, plasmids can impose fitness costs on the host, lowering their growth rate (Carroll and Wong, 2018; San Millan and

---

J.B. Alderliesten, M.P. Zwart, J. Arjan G.M. de Visser et al.

Journal of Theoretical Biology 533 (2022) 110937

MacLean, 2017). Results of mathematical modelling indicate that despite such costs, plasmids can invade well-mixed populations of plasmid-free bacteria by conjugation under a broad range of conditions (Lopatkin et al., 2017; Stewart and Levin, 1977).

Most mathematical models of plasmid dynamics follow the original model of Levin *et al.* (Levin et al., 1979) and assume mass-action kinetics of conjugation in well-mixed populations (Leclerc et al., 2019). Since plasmid-bearing bacteria (donors) need to form pairs with plasmid-free bacteria (recipients) for conjugation to occur, and pair formation may limit conjugation rates, this model has been extended to explicitly model pair formation (Zhong et al., 2010). Pairs of bacteria detach faster during conjugation in suspension as mixing is intensified, because the increased shear force breaks the fragile conjugative pili that connect pairs of bacteria (Zhong et al., 2010). In contrast, pairs of bacteria adhering to surfaces are stabilized by their fixed location, potentially leading to higher pair-formation rates or lower detachment rates on surfaces than in liquids (Alderliesten et al., 2020; Licht et al., 1999).

These differences in pair formation could play an important role in environments where bacteria can migrate between liquid environments and surfaces such as the animal gut wall (Freter et al., 1983b), solid particles in wastewater treatment plants (Zhao et al., 2019), and chemostat vessel walls (Stemmons and Smith, 2000). Higher attachment rates or lower detachment rates at such surfaces could increase the number of transconjugants (i.e., recipient bacteria that have received a plasmid) produced by one invading donor bacterium. Additionally, migration to a surface where turnover is lower than in the liquid environment prolongs the time an invading donor spends in the system before being washed out, which also could increase the number of transconjugants produced by an invading donor bacterium.

The effect of different pair-formation kinetics in the lumen and at the wall on the invasion dynamics of plasmids has so far been neglected. To fill this gap, we extend the one-compartment pair-formation model (Zhong et al., 2010) to a two-compartment model (Imran et al., 2005), with a liquid compartment representing the gut lumen and a surface-like compartment representing the gut wall, respectively. Our extended model includes inflow of nutrients, washout of nutrients and bacteria, and different attachment and detachment rates in the two compartments. We also compare the pair-formation models with bulk-conjugation models to investigate if they lead to different parameter spaces for invasion, or to other dynamics over time. We use mathematical models to be able to change model parameters that are not easy to manipulate *in vivo* and to quantify how sensitive the model is to uncertainty in the parameter values, to identify for which parameters accurate estimates are needed.

2. Methods

2.1. Overview of the models

In this section, we will first introduce models consisting of a single compartment. After describing the nutrient flow and bacterial growth, we will describe conjugation in a bulk-conjugation model and conjugation in a pair-formation model (Fig. 1A, C). The pair-formation model explicitly describes the formation of pairs of bacteria in which conjugation takes place, whereas the bulk-conjugation model assumes instantaneous transfer of the plasmid at contact. Next, we will extend these one-compartment models to two-compartment models with bacteria migrating between the compartments (Fig. 1B, D). The used variables and parameters are given in Table 1, together with a description, their units, and the default values used in the numerical simulations.

2.2. One-compartment models

2.2.1. Flow, nutrients, and bacterial growth

We assume chemostat-like dynamics, where the inflowing liquid contains φ mg nutrients $\cdot$ mL^{-1}, flows through the system with washout rate ρ h^{-1} and carries bacteria and remaining nutrients at the outflow. Nutrient uptake is modelled with a Monod function with K_s mg limiting nutrients $\cdot$ mL^{-1} as half-saturation constant, maximal growth rate ψ h^{-1}, and ε mg nutrients used per cell division. The growth rate of plasmid-bearing bacteria is modelled by multiplying the recipient growth rate ψ h^{-1} by $1 - c_D$ for donors and by $1 - c_T$ for transconjugants, with c_D and c_T being dimensionless numbers between 0 and 1 indicating fitness costs of plasmid carriage and, for the donors, additional costs of being in a new environment. Bacteria in a pair grow at the same rate as their single-celled counterparts, but their offspring is added to the appropriate single-celled populations, not to the pairs.

2.2.2. One-compartment bulk-conjugation model

The bulk-conjugation model (Equation 1) describes the change in the concentration of nutrients (S), recipients (R; defined here as bacteria that do not carry the plasmid of interest), donors (D), and transconjugants (T) over time, with differentiation with respect to time indicated by a dot (˙). Conjugation is modelled as a nutrient-independent instantaneous mass-action process with bulk-conjugation rates γ_D^{bulk} (mL $\cdot$ cell^{-1} $\cdot$ h^{-1}) for donors and γ_T^{bulk} (mL $\cdot$ cell^{-1} $\cdot$ h^{-1}) for transconjugants, where conjugation is proportional to the densities of plasmid-free and plasmid-bearing bacteria.

2.2.2.1. Model equations.

$$\dot{S} = (\varphi - S)\rho - \frac{\epsilon\psi S}{K_s + S}(R + (1 - c_D)D + (1 - c_T)T) \quad (1a)$$

$$\dot{R} = \left(\frac{\psi S}{K_s + S} - \gamma_D^{bulk}D - \gamma_T^{bulk}T - \rho\right)R \quad (1b)$$

$$\dot{D} = \left(\frac{\psi(1 - c_D)S}{K_s + S} - \rho\right)D \quad (1c)$$

$$\dot{T} = \left(\frac{\psi(1 - c_T)S}{K_s + S} + \gamma_T^{bulk}R - \rho\right)T + \gamma_D^{bulk}RD \quad (1d)$$

2.2.3. One-compartment pair-formation model

The pair-formation model (Equation 2) describes the change in the concentration of nutrients (S), recipients (R), donors (D), transconjugants (T), recipient-donor pairs (M_{RD}), recipient-transconjugant pairs (M_{RT}), donor-transconjugant pairs (M_{DT}) and transconjugant-transconjugant pairs (M_{TT}) over time. We only consider pair formation between plasmid-free (R) and plasmid-bearing (D, T) bacteria, such that M_{DT} and M_{TT} pairs are only formed after conjugation in M_{RD} and M_{RT} pairs, not through pair formation of a single transconjugant with a donor or another transconjugant. Pair formation between bacteria is modelled as a mass-action process with attachment rate κ_+ (mL $\cdot$ cell^{-1} $\cdot$ h^{-1}), where attachment is proportional to the densities of plasmid-free and plasmid-bearing bacteria (Zhong et al., 2010). Pairs of bacteria detach into single cells with detachment rate κ_- (h^{-1}). Conjugation is modelled as a nutrient-independent process that occurs in recipient-donor pairs with intrinsic conjugation rate γ_D (h^{-1}) and in recipient-transconjugant pairs with intrinsic conjugation rate γ_T (h^{-1}).
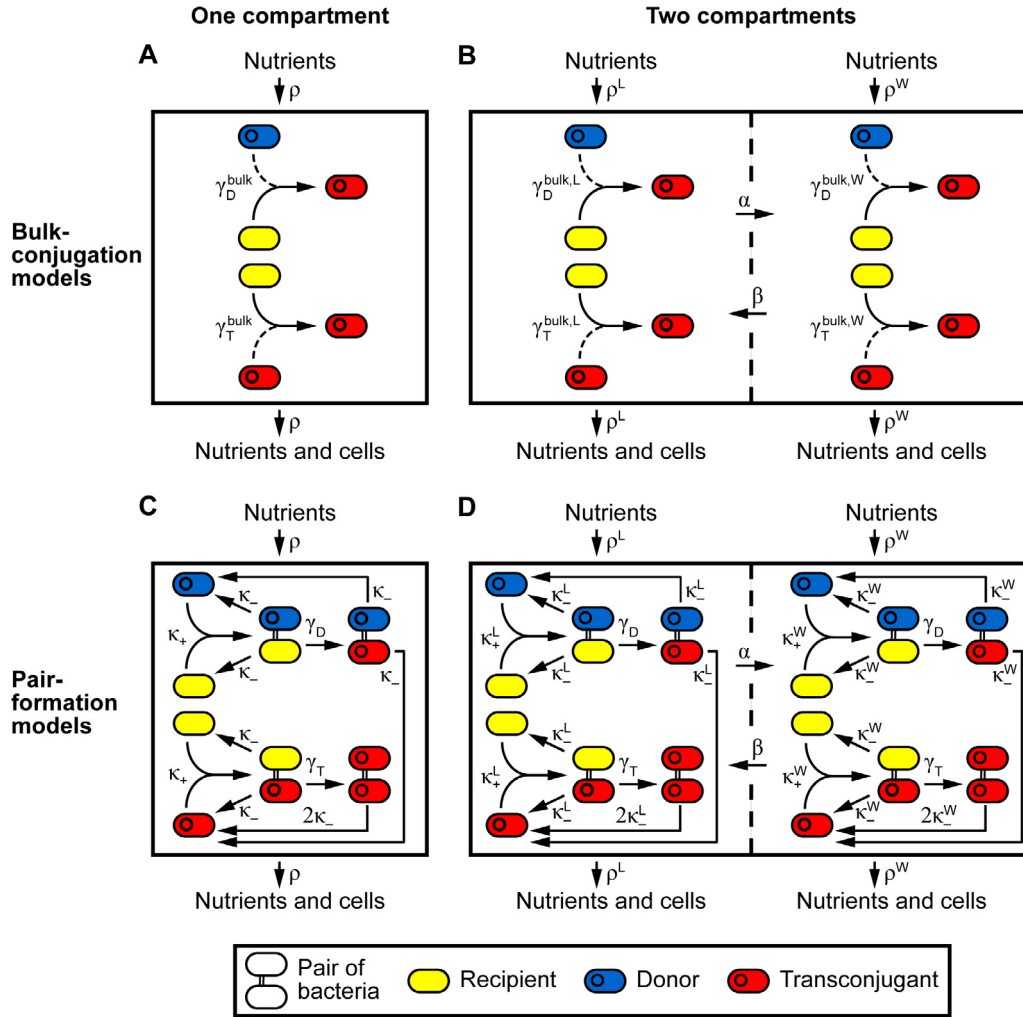
Fig. 1. Flow diagrams for the four models describing conjugation. Boxes describe the densities of donors, recipients, transconjugants and pairs of bacteria, solid arrows indicate conversion to another type of bacterium and dashed arrows indicate bacteria that contribute to mass-action processes without being converted. Vertical dashed lines in the two-compartment models separate the lumen and the wall, which have their own washout, bulk-conjugation, attachment, and detachment rates. Nutrients enter the system at a constant rate ρ and are used for cell division (not shown), cells and unused nutrients wash out. **A** One-compartment bulk-conjugation model. **B** Two-compartment bulk-conjugation model consisting of a lumen (L) and a wall (W) compartment. **C** One-compartment pair-formation model. **D** Two-compartment pair-formation model consisting of a lumen (L) and a wall (W) compartment. Abbreviations: α: migration rate to the wall (h^{-1}); β: migration rate to the lumen (h^{-1}); γ_D and γ_T: intrinsic conjugation rates of the donor and transconjugant in pairs with a recipient (h^{-1}); γ_D^{bulk} and γ_T^{bulk}: bulk-conjugation rates of the donor and transconjugant (mL $\cdot$ cell^{-1} $\cdot$ h^{-1}); κ_-: detachment rate (h^{-1}); κ_+: attachment rate (mL $\cdot$ cell^{-1} $\cdot$ h^{-1}); ρ: washout rate (h^{-1}); L: lumen compartment; W: wall compartment.

2.2.3.1. Model equations.

$$\dot{S} = (\varphi - S)\rho - \frac{\epsilon\psi S}{K_s + S}(R + M_{RD} + M_{RT} + (1 - c_D)(D + M_{RD} + M_{DT})$$
$$+ (1 - c_T)(T + M_{RT} + M_{DT} + 2M_{TT})) \tag{2a}$$

$$\dot{R} = \frac{\psi S}{K_s + S}(R + M_{RD} + M_{RT}) - (\kappa_+(D + T) + \rho)R$$
$$+ \kappa_-(M_{RD} + M_{RT}) \tag{2b}$$

$$\dot{D} = \frac{\psi(1 - c_D)S}{K_s + S}(D + M_{RD} + M_{DT}) - (\kappa_+ R + \rho)D$$
$$+ \kappa_-(M_{RD} + M_{DT}) \tag{2c}$$

$$\dot{T} = \frac{\psi(1 - c_T)S}{K_s + S}(T + M_{RT} + M_{DT} + 2M_{TT}) - (\kappa_+ R + \rho)T$$
$$+ \kappa_-(M_{RT} + M_{DT} + 2M_{TT}) \tag{2d}$$

$$\dot{M}_{RD} = \kappa_+ RD - (\kappa_- + \rho + \gamma_D)M_{RD} \tag{2e}$$

$$\dot{M}_{RT} = \kappa_+ RT - (\kappa_- + \rho + \gamma_T)M_{RT} \tag{2f}$$

$$\dot{M}_{DT} = \gamma_D M_{RD} - (\kappa_- + \rho)M_{DT} \tag{2g}$$

$$\dot{M}_{TT} = \gamma_T M_{RT} - (\kappa_- + \rho)M_{TT} \tag{2h}$$

2.3. Two-compartment models

In the two-compartment models, we consider the gut lumen (L) and the gut wall (W) as two compartments equivalent to the one-compartment models, between which bacteria can migrate.

2.3.1. Flow, nutrients, bacterial growth and migration

Nutrients are modelled separately in the lumen and at the wall. This allows us to obtain the same nutrient concentration and cell density in the lumen and at the wall as in the one-compartment model. We assume the lumen and the wall have their own washout rate (ρ^L and ρ^W h^{-1}) and nutrient concentration at the inflow (φ^L

J.B. Alderliesten, M.P. Zwart, J. Arjan G.M. de Visser et al.

Journal of Theoretical Biology 533 (2022) 110937

Table 1
Variables and parameters of the models.

Variable or parameter	Description	(Initial) value	Units	References and notes
Initial values of the variables				
S, S^L, S^W	Nutrient concentration	$1.6 \cdot 10^{-4}$	$mg \cdot mL^{-1}$	At plasmid-free equilibrium
R, R^L, R^W	Recipient concentration	$1 \cdot 10^7$	$cell \cdot mL^{-1}$	At plasmid-free equilibrium; see Table A.1
D, D^L	Donor concentration	1000	$cell \cdot mL^{-1}$	Invasion-when-rare
D^W	Donor concentration at the wall	0	$cell \cdot mL^{-1}$	Invasion from the lumen
T, T^L, T^W	Transconjugant concentration	0	$cell \cdot mL^{-1}$	–
$M_{RD}, M_{RD}^L, M_{RD}^W$	Recipient-donor pair concentration	0	$cell \cdot mL^{-1}$	–
$M_{RT}, M_{RT}^L, M_{RT}^W$	Recipient-transconjugant pair concentration	0	$cell \cdot mL^{-1}$	–
$M_{DT}, M_{DT}^L, M_{DT}^W$	Donor-transconjugant pair concentration	0	$cell \cdot mL^{-1}$	–
$M_{TT}, M_{TT}^L, M_{TT}^W$	Transconjugant pair concentration	0	$cell \cdot mL^{-1}$	–
Parameter values				
φ, φ^L	Nutrient concentration in the inflowing liquid	1.4	$mg \cdot mL^{-1}$	(Mitchell and Lemme, 2008; Savory and Mitchell, 1991) [a][b]
φ^W	Nutrient concentration in the inflowing liquid	1.4	$mg \cdot mL^{-1}$	
ρ, ρ^L, ρ^W	Washout rate	0.029	h^{-1}	50% remaining after 24 h [a]
ϵ	Nutrient conversion ratio	$1.4 \cdot 10^{-7}$	$mg \cdot cell^{-1}$	To obtain 10^7 cells $\cdot mL^{-1}$ at equilibrium [a]
ψ	Maximum growth rate	0.738	h^{-1}	(Stewart and Levin, 1977)
K_s	Half-saturation constant	0.004	mg limiting nutrient $\cdot mL^{-1}$	(Stewart and Levin, 1977)
c_D	Fitness costs in donor	0.18	–	Higher than costs in transconjugant [a]
c_T	Fitness costs in transconjugant	0.09	–	(Vogwill and MacLean, 2015)
$\kappa_+, \kappa_+^L, \kappa_+^W$	Attachment rate	$10^{-12} - 10^{-8}$	$mL \cdot cell^{-1} \cdot h^{-1}$	(Zhong et al., 2010)
$\kappa_-, \kappa_-^L, \kappa_-^W$	Detachment rate	$10^{-1} - 10^3$	h^{-1}	(Zhong et al., 2010) reports $0 - 5 \cdot 10^3$
γ_D, γ_T	Intrinsic conjugation rates of donor and transconjugant	15	h^{-1}	(Zhong et al., 2010)
$\gamma_D^{bulk}, \gamma_D^{bulk,L}, \gamma_D^{bulk,W}, \gamma_T^{bulk}, \gamma_T^{bulk,L}, \gamma_T^{bulk,W}$	Bulk-conjugation rates of donor and transconjugant	Various	$mL \cdot cell^{-1} \cdot h^{-1}$	Estimated from pair-formation models [a]
α	Migration rate from the lumen to the wall	0.1	h^{-1}	(Imran et al., 2005) [a]
β	Migration rate from the wall to the lumen	0.1	h^{-1}	(Imran et al., 2005) [a]

[a] Value not determined experimentally.
[b] To obtain the same nutrient concentration and cell density in the lumen and at the wall as in the one-compartment model.

and φ^W mg nutrients $\cdot mL^{-1}$). Washout from the wall is modified by including ρ_S^W (h^{-1}) as a separate washout term for nutrients, to be able to exclude washout of bacteria from the wall, while still allowing the flow of nutrients. Nutrient uptake and growth are modelled in the same way as in the one-compartment model. Bacteria migrate from the lumen to the wall with rate α (h^{-1}), and from the wall to the lumen with rate β (h^{-1}). The migration rates are assumed not to be affected by bearing a plasmid or being in a pair.

2.3.2. Two-compartment bulk-conjugation model

In the two-compartment bulk-conjugation model (Equation 3), conjugation is instantaneous as in the one-compartment model. The bulk-conjugation rates can differ between the two compartments as a result of differences in attachment and detachment rates.

2.3.2.1. Model equations.

$$\dot{S}^L = \left(\varphi^L - S^L\right)\rho^L - \frac{\epsilon\psi S^L}{K_s + S^L}\left(R^L + (1 - c_D)D^L + (1 - c_T)T^L\right) \quad (3a)$$

$$\dot{R}^L = \left(\frac{\psi S^L}{K_s + S^L} - \rho^L - \alpha\right)R^L + \beta R^W - \left(\gamma_D^{bulk,L}D^L + \gamma_T^{bulk,L}T^L\right)R^L \quad (3b)$$

$$\dot{D}^L = \left(\frac{\psi(1 - c_D)S^L}{K_s + S^L} - \rho^L - \alpha\right)D^L + \beta D^W \quad (3c)$$

$$\dot{T}^L = \left(\frac{\psi(1 - c_T)S^L}{K_s + S^L} - \rho^L - \alpha\right)T^L + \beta T^W + \left(\gamma_D^{bulk,L}D^L + \gamma_T^{bulk,L}T^L\right)R^L \quad (3d)$$

$$\dot{S}^W = \left(\varphi^W - S^W\right)\rho_S^W - \frac{\epsilon\psi S^W}{K_s + S^W}\left(R^W + (1 - c_D)D^W + (1 - c_T)T^W\right) \quad (3e)$$

$$\dot{R}^W = \left(\frac{\psi S^W}{K_s + S^W} - \rho^W - \beta\right)R^W + \alpha R^L - \left(\gamma_D^{bulk,W}D^W + \gamma_T^{bulk,W}T^W\right)R^W \quad (3f)$$

$$\dot{D}^W = \left(\frac{\psi(1 - c_D)S^W}{K_s + S^W} - \rho^W - \beta\right)D^W + \alpha D^L \quad (3g)$$

$$\dot{T}^W = \left(\frac{\psi(1 - c_T)S^W}{K_s + S^W} - \rho^W - \beta\right)T^W + \alpha T^L + \left(\gamma_D^{bulk,W}D^W + \gamma_T^{bulk,W}T^W\right)R^W \quad (3h)$$

2.3.3. Two-compartment pair-formation model

In the two-compartment pair-formation model (Equation 4), pair formation is modelled as in the one-compartment model. The attachment and detachment rates can differ between the two compartments to describe differences in pair-formation and conjugation kinetics between the lumen and the wall.

J.B. Alderliesten, M.P. Zwart, J. Arjan G.M. de Visser et al.

Journal of Theoretical Biology 533 (2022) 110937

2.3.3.1. Model equations.

$$\dot{S}^L = \left(\varphi^L - S^L\right)\rho^L - \frac{\epsilon\psi S^L}{K_s + S^L}\left(R^L + M_{RD}^L + M_{RT}^L + (1-c_D)\left(D^L + M_{RD}^L + M_{DT}^L\right)\right.$$
$$\left. + (1-c_T)\left(T^L + M_{RT}^L + M_{DT}^L + 2M_{TT}^L\right)\right) \tag{4a}$$

$$\dot{R}^L = \frac{\psi S^L}{K_s + S^L}\left(R^L + M_{RD}^L + M_{RT}^L\right) - \left(\rho^L + \alpha + \kappa_+^L\left(D^L + T^L\right)\right)R^L$$
$$+ \kappa_-^L\left(M_{RD}^L + M_{RT}^L\right) + \beta R^W \tag{4b}$$

$$\dot{D}^L = \frac{\psi(1-c_D)S^L}{K_s + S^L}\left(D^L + M_{RD}^L + M_{DT}^L\right) - \left(\rho^L + \alpha + \kappa_+^L R^L\right)D^L$$
$$+ \kappa_-^L\left(M_{RD}^L + M_{DT}^L\right) + \beta D^W \tag{4c}$$

$$\dot{T}^L = \frac{\psi(1-c_T)S^L}{K_s + S^L}\left(T^L + M_{RT}^L + M_{DT}^L + 2M_{TT}^L\right)$$
$$- \left(\rho^L + \alpha + \kappa_+^L R^L\right)T^L + \kappa_-^L\left(M_{RT}^L + M_{DT}^L + 2M_{TT}^L\right) + \beta T^W \tag{4d}$$

$$\dot{M}_{RD}^L = \kappa_+^L R^L D^L - \left(\kappa_-^L + \gamma_D + \rho^L + \alpha\right)M_{RD}^L + \beta M_{RD}^W \tag{4e}$$

$$\dot{M}_{RT}^L = \kappa_+^L R^L T^L - \left(\kappa_-^L + \gamma_T + \rho^L + \alpha\right)M_{RT}^L + \beta M_{RT}^W \tag{4f}$$

$$\dot{M}_{DT}^L = \gamma_D^L M_{RD}^L - \left(\kappa_-^L + \rho^L + \alpha\right)M_{DT}^L + \beta M_{DT}^W \tag{4g}$$

$$\dot{M}_{TT}^L = \gamma_T^L M_{RT}^L - \left(\kappa_-^L + \rho^L + \alpha\right)M_{TT}^L + \beta M_{TT}^W \tag{4h}$$

$$\dot{S}^W = \left(\varphi^W - S^W\right)\rho_S^W$$
$$- \frac{\epsilon\psi S^W}{K_s + S^W}\left(R_W + M_{RD}^W + M_{RT}^W + (1-c_D)\left(D^W + M_{RD}^W + M_{DT}^W\right)\right.$$
$$\left. + (1-c_T)\left(T^W + M_{RT}^W + M_{DT}^W + 2M_{TT}^W\right)\right) \tag{4i}$$

$$\dot{R}^W = \frac{\psi S^W}{K_s + S^W}\left(R^W + M_{RD}^W + M_{RT}^W\right)$$
$$- \left(\rho^W + \beta + \kappa_+^W\left(D^W + T^W\right)\right)R^W + \kappa_-^W\left(M_{RD}^W + M_{RT}^W\right)$$
$$+ \alpha R^L \tag{4j}$$

$$\dot{D}^W = \frac{\psi(1-c_D)S^W}{K_s + S^W}\left(D^W + M_{RD}^W + M_{DT}^W\right)$$
$$- \left(\rho^W + \beta + \kappa_+^W R_W\right)D^W + \kappa_-^W\left(M_{RD}^W + M_{DT}^W\right) + \alpha D^L \tag{4k}$$

$$\dot{T}^W = \frac{\psi(1-c_T)S^W}{K_s + S^W}\left(T^W + M_{RT}^W + M_{DT}^W + 2M_{TT}^W\right)$$
$$- \left(\rho^W + \beta + \kappa_+^W R^W\right)T^W + \kappa_-^W\left(M_{RT}^W + M_{DT}^W + 2M_{TT}^W\right)$$
$$+ \alpha T^L \tag{4l}$$

$$\dot{M}_{RD}^W = \kappa_+^W R^W D^W - \left(\kappa_-^W + \gamma_D + \rho^W + \beta\right)M_{RD}^W + \alpha M_{RD}^L \tag{4m}$$

$$\dot{M}_{RT}^W = \kappa_+^W R^W T^W - \left(\kappa_-^W + \gamma_T + \rho^W + \beta\right)M_{RT}^W + \alpha M_{RT}^L \tag{4n}$$

$$\dot{M}_{DT}^W = \gamma_D^W M_{RD}^W - \left(\kappa_-^W + \rho^W + \beta\right)M_{DT}^W + \alpha M_{DT}^L \tag{4o}$$

$$\dot{M}_{TT}^W = \gamma_T^W M_{RT}^W - \left(\kappa_-^W + \rho^W + \beta\right)M_{TT}^W + \alpha M_{TT}^L \tag{4p}$$

2.4. Estimating bulk-conjugation rates to compare models

Transconjugants should be formed at the same rate in the bulk-conjugation model and in the pair-formation model to be able to compare the predictions of these models. This indicates the bulk-conjugation rates of donors and transconjugants can be calculated using (Zhong et al., 2010):

$$\gamma_D^{bulk} R_{total} D_{total} = \gamma_D M_{RD} \rightarrow \gamma_D^{bulk} = \frac{\gamma_D M_{RD}}{R_{total} D_{total}} \tag{5}$$

$$\gamma_T^{bulk} R_{total} T_{total} = \gamma_T M_{RT} \rightarrow \gamma_T^{bulk} = \frac{\gamma_T M_{RT}}{R_{total} T_{total}} \tag{6}$$

The densities of the different populations that are needed for this calculation are taken from the output of short-term simulations with adjusted pair-formation models that only include pair formation and conjugation (Section 3 in the appendix). Excluding growth, and thus the effect of plasmid costs on growth, ensures the estimates of the bulk-conjugation rates are not influenced by plasmid costs. Excluding washout prevents plasmid-bearing populations from vanishing if the plasmid cannot invade, which ensures more stable estimates of the bulk-conjugation rates.

2.5. Model scenarios

To determine if the plasmid can invade a population of plasmid-free bacteria at equilibrium, the eigenvalues of the Jacobian matrix of the system of ordinary differential equations are numerically calculated at the plasmid-free equilibrium. If all eigenvalues have negative real parts, the system will return to the plasmid-free equilibrium after perturbation by a plasmid-bearing bacterium, such that the plasmid cannot invade. If, in contrast, any of the eigenvalues have a positive real part, the system will move away from the plasmid-free equilibrium after perturbation by a plasmid-bearing bacterium, such that the plasmid can invade (Edelstein-Keshet, 2005).

This analysis is performed for different parameter values to assess their influence on the stability of the plasmid-free equilibrium. For the one-compartment pair-formation model, we assess the influence of the nutrient concentration at the inflow, washout rate, plasmid costs, and conjugation rate. For the two-compartment pair-formation model, we first restrict our analyses to cases where the cell densities at the plasmid-free equilibrium are the same in the lumen and at the wall, by using identical washout rates and nutrient concentrations at the inflow for the two compartments, and by using identical migration rates for migration from the lumen to the wall and vice versa. As a consequence, the two compartments only differ in their attachment and detachment rates. Next, we analyse the effect of different cell densities in the lumen and at the wall, by excluding washout of bacteria from the wall and using different migration rates from the lumen to the wall and vice versa. We also compare predictions of the different models. First, we compare predictions of the one-compartment pair-formation model with predictions of the two-compartment pair-formation model in cases where either (1) the density, attachment rates, and detachment rates in the lumen are equal to those at the wall, (2) the density is higher at the wall than in the lumen because washout from the wall is excluded, but the attachment rates and detachment rates in the lumen and at the wall are equal, and (3) the density in the lumen and at the wall are equal, but the attachment rate at the wall is high (10^{-9} mL $\cdot$ cell^{-1} $\cdot$ h^{-1}) and the detachment rate at the wall is low (10^{-1} h^{-1}). Finally, we compare

J.B. Alderliesten, M.P. Zwart, J. Arjan G.M. de Visser et al.

Journal of Theoretical Biology 533 (2022) 110937

predictions of the pair-formation models with predictions of the bulk-conjugation models.

2.6. Model parameterization and description of variables and parameters

The default values for the variables and parameters are given in Table 1. The recipient density of $1 \cdot 10^7$ cells $\cdot$ mL^{-1} at the plasmid-free equilibrium reflects the density of *Escherichia coli* in the lumen of the chicken caecum (Table A.1) and is obtained by adjusting the nutrient conversion ratio. The initial donor concentration of 1000 cells $\cdot$ mL^{-1} concerns the starting point for the simulations over time. The nutrient concentration in the inflowing liquid of the lumen is based on the glucose concentration in the ileum of broiler chickens. Nutrients are modelled separately in the lumen and at the wall. This allows us to obtain the same nutrient concentration and cell density in the lumen, at the wall, and in the one-compartment model. The washout rate of 0.029 h^{-1} is based on 50% of the population remaining after 24 h. Fitness costs are assumed to be higher in the donor than in the transconjugant because donors experience costs of being in a new environment in addition to costs of bearing a plasmid.

2.7. Software and source code

All calculations were performed in R version 4.1.1 (R Core Team, 2020). The stability of the plasmid-free equilibria was determined using the rootSolve package version 1.8.2.2 (Soetaert, 2009). Model simulations showing dynamics over time were performed using the deSolve package version 1.28 (Soetaert et al., 2010). Plots were created using the ggplot2-package version 3.3.5 (Wickham, 2016).

Fig. 2. One-compartment pair-formation model: the ability of the plasmid to invade (yellow area) for a range of parameter values affecting the recipient density and time spent in the system. Different facets show increasing nutrient concentrations at the inflow (left to right), and increasing washout rates (top to bottom). Individual facets show increasing attachment rates from left to right and decreasing detachment rates from top to bottom. The default values as listed in Table 1 have been used for the other parameters.

R-code is provided at the GitHub-repository https://github.com/EgilFischer/MITAR.git.

3. Results

3.1. One-compartment pair-formation model

We first consider plasmid invasion as predicted with the pair-formation model with a single gut compartment. For a given combination of nutrient concentration and washout rates, the attachment rate needs to exceed a threshold depending on the detachment rate to enable invasion of a plasmid (Fig. 2). The plasmid can invade in 28% of the combinations of attachment and detachment rates if the default parameter values listed in Table 1 are used (Fig. 2). Decreasing the nutrient concentration in the inflowing liquid to 0.14 mg·mL^{-1} decreases the recipient density such that the plasmid can invade in only 8% of the parameter combinations. Increasing the nutrient concentration to 14 mg·mL^{-1} increases the recipient density such that the plasmid can invade in 52% of the parameter combinations. Decreasing the washout rate to 0.0029 h^{-1} prolongs the time bacteria spend in the system before being washed out such that the plasmid can invade in 52% of the parameter combinations. Increasing the washout rate to 0.29 h^{-1} shortens the time bacteria spend in the system such that
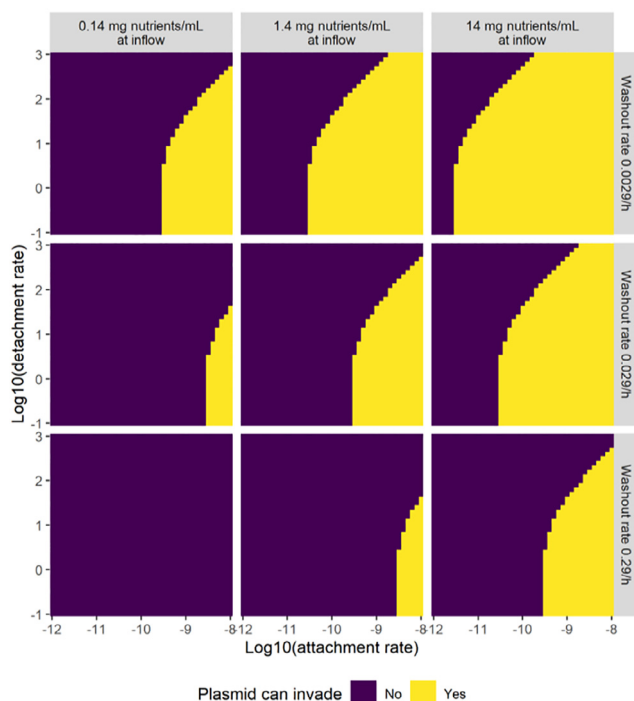

Fig. 3. One-compartment pair-formation model: the percentage of attachment rates for which the plasmid can invade for different fitness costs and intrinsic conjugation rates of the transconjugant (left to right) and increasing washout rates (top to bottom). Individual facets show increasing nutrient concentrations at the inflow from left to right and decreasing detachment rates from top to bottom. The default values as listed in Table 1 have been used for the other parameters.
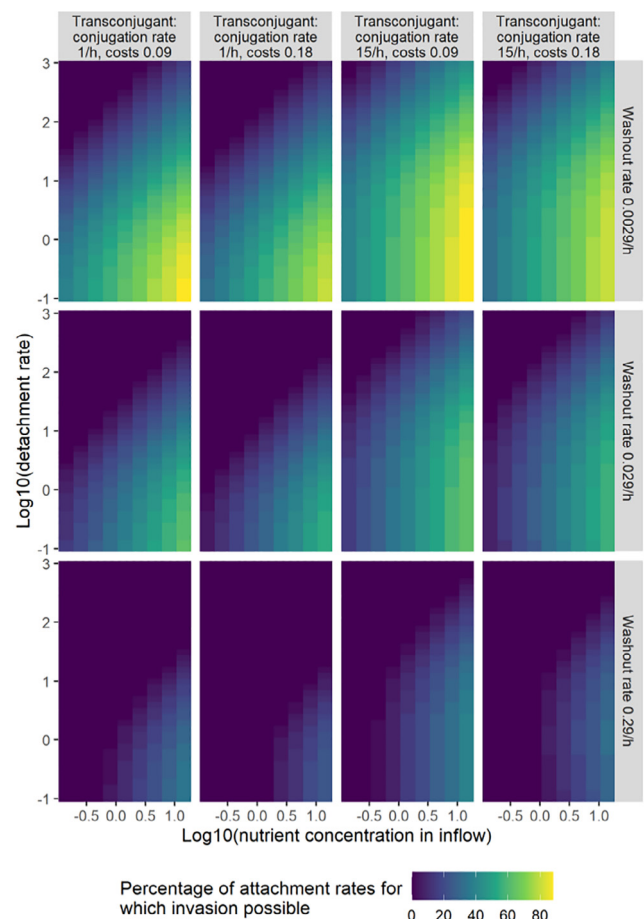
the plasmid can invade in only 8% of the parameter combinations (Fig. 2).

Increasing plasmid costs of the transconjugants to 0.18 decreases transconjugant fitness, lowering the percentage of attachment rates for which invasion is possible (Fig. 3). Decreasing the intrinsic conjugation rate of the transconjugants to 1 h⁻¹ also lowers this percentage (Fig. 3). In contrast, the costs and intrinsic conjugation rates of the donors do not influence the range of conditions where invasion is possible (Fig. A.5 and Section 6 of the supplement). This difference is explained by the choice for donors and transconjugants that always have lower fitness than recipients (c_D, $c_T > 0$), combined with the fact that conjugation leads to new transconjugants but not to new donors, such that transconjugants can overcome their costs with conjugation, whereas donors cannot.

3.2. Two-compartment pair-formation model

Next, we consider plasmid invasion as predicted with the pair-formation model with two compartments. The plasmid can invade if the attachment rate is high enough and the detachment rate low enough in the lumen, at the wall, or in both compartments (bottom right-hand, top left-hand, and top right-hand parts of facets in Fig. 4 respectively). We first restrict our analyses to cases where the cell densities at the plasmid-free equilibrium in the lumen and the wall are equal. Then equal detachment rates in the lumen and at the wall lead to equal thresholds which the attachment rates in the lumen and at the wall have to exceed to enable invasion of the plasmid, hence the symmetry in the facets on the diagonal in Fig. 4. For detachment rates of 0.1 and 10 in the first two of those facets, the plasmid can invade 55% and 48% of the combinations of attachment rates in the lumen and attachment rates at the
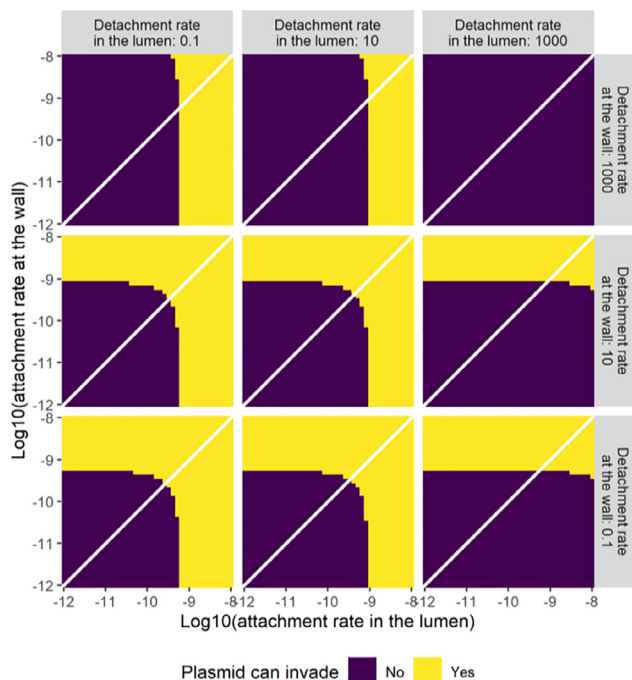

Fig. 4. Two-compartment model with equal cell densities: the ability of the plasmid to invade (yellow area) for increasing detachment rates in the lumen (left to right) and increasing detachment rates at the wall (bottom to top) when the cell densities at the plasmid-free equilibrium are the same in the lumen and at the wall. Individual facets show increasing attachment rates in the lumen (left to right) and increasing attachment rates at the wall (bottom to top). The default values as listed in Table 1 have been used for the other parameters. The white diagonals indicate where the attachment rates in the lumen are equal to the attachment rates at the wall.
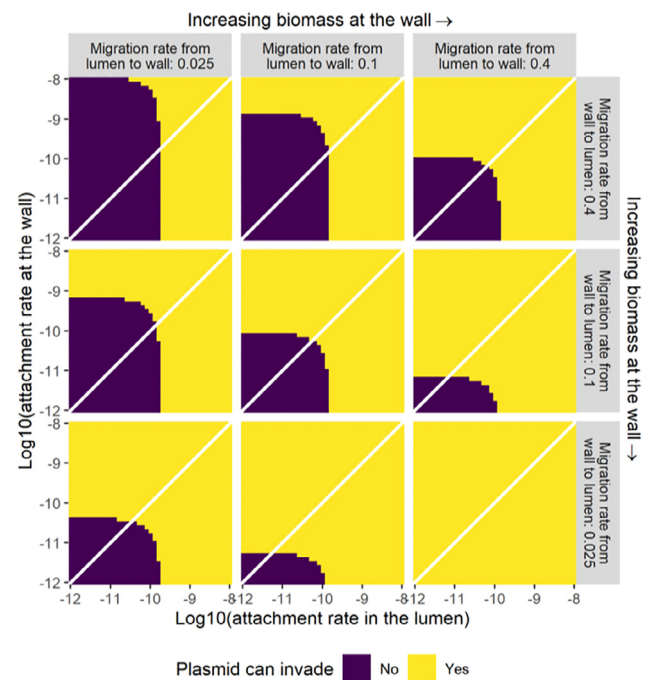

Fig. 5. Two-compartment model with unequal cell densities: the ability of the plasmid to invade (yellow area) for increasing migration rates from the lumen to the wall (left to right) and increasing migration rates from the wall to the lumen (bottom to top) when detachment rates in the lumen and at the wall are both fixed at 0.1 h⁻¹ and washout from the wall is excluded. Individual facets show increasing attachment rates in the lumen from left to right and increasing attachment rates at the wall from bottom to top. The default values as listed in Table 1 have been used for the other parameters. The arrows above and at the right-hand side of the plot indicate increasing density at the wall caused by the migration rates. The white diagonals indicate where the attachment rates in the lumen are equal to the attachment rates at the wall.

wall, respectively. These facets also show the plasmid can invade despite low attachment rates in the lumen (e.g., 10⁻¹²) if the attachment rate at the wall is high enough (i.e., 10⁻⁹·² or higher and 10⁻⁹ and higher). If the detachment rates are increased to 10³, the plasmid cannot invade for any of the used parameter combinations.

Now we continue our analyses of the two-compartment model with cases where the cell densities at the plasmid-free equilibria in the lumen and the wall differ from each other. The density at the wall increases if the migration rate from the lumen to the wall increases or if the migration rate from the wall to the lumen decreases. The increased density at the wall, combined with mass-action dynamics for attachment and conjugation, enables invasion of the plasmid for low values of the attachment rates in the lumen and at the wall (bottom left-hand part of facets in Fig. 5). Invasion is not possible for these low attachment rates when the density at the wall is lower than, or equal to, the density in the lumen (facets on and above the diagonal of Fig. 5).

3.3. Comparing one- and two-compartment pair-formation models

Now we compare plasmid invasion as predicted by the one-compartment pair-formation model and the two-compartment pair-formation model. If the density, attachment rates, and detachment rates in the one-compartment model are the same as those in the lumen and at the wall of the two-compartment model, both models predict the same parameter space for plasmid invasion, and invasion is possible in 28% of the parameter combinations (Fig. 6A, B). However, if the density at the wall is larger than the density in the lumen because washout from the wall is excluded,
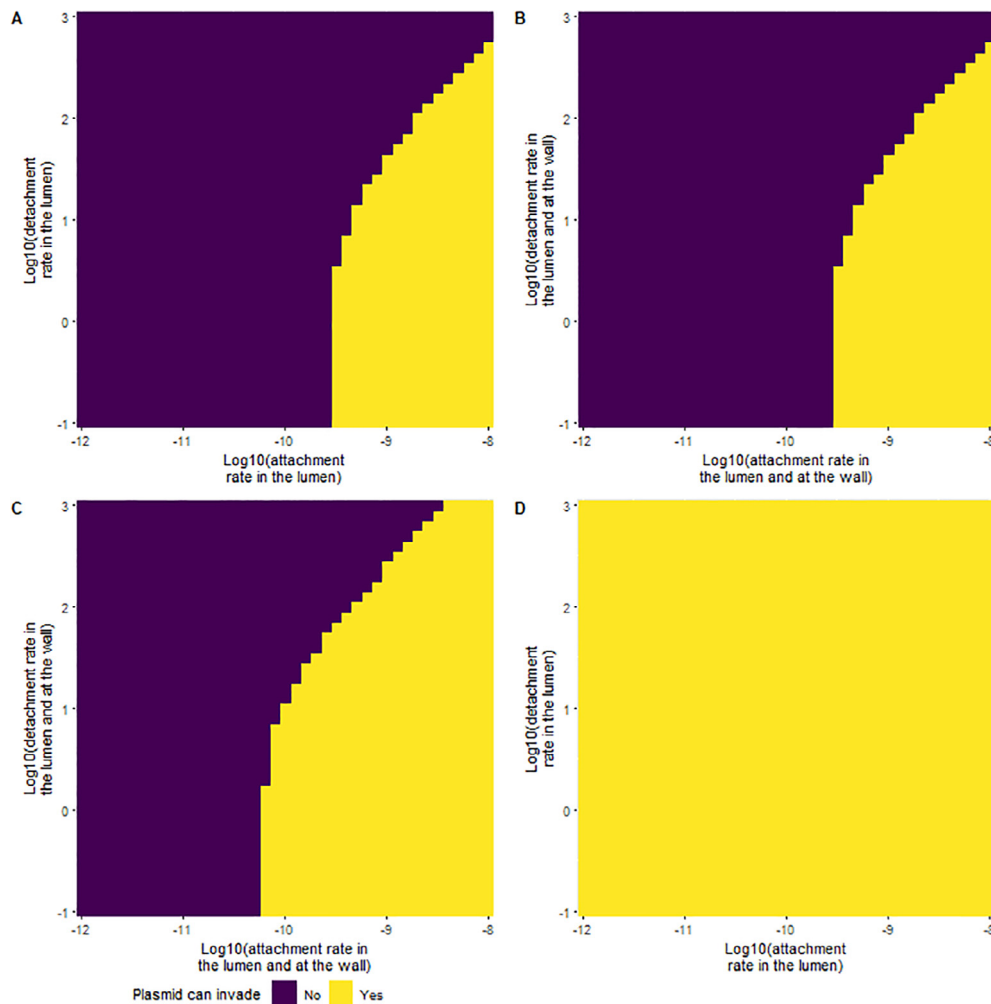
J.B. Alderliesten, M.P. Zwart, J. Arjan G.M. de Visser et al.

Journal of Theoretical Biology 533 (2022) 110937

Fig. 6. The ability of the plasmid to invade (yellow area) for increasing attachment rates (left to right) and increasing detachment rates (bottom to top) in the one-compartment model (A), in the two-compartment model where density, attachment rates, and detachment rates in the lumen are equal to those at the wall (B), in the two-compartment model where attachment rates and detachment rates in the lumen are equal to those at the wall, but the density at the wall is higher than the density in the lumen because washout from the wall is excluded (C), and in the two-compartment model where density in the lumen is equal to the density at the wall, but the attachment rate at the wall is fixed at a high value (10^{-9} mL $\cdot$ cell^{-1} $\cdot$ h^{-1}) and the detachment rate at the wall is fixed to a low value (10^{-1}h^{-1}; D). The default values as listed in Table 1 have been used for the other parameters.

the parameter space for invasion is wider in the two-compartment model than in the one-compartment model, and invasion is possible in 44% of the parameter combinations in the two-compartment model (Fig. 6C). If the density at the wall is equal to the density in the lumen, but the attachment rate at the wall is fixed at a high value (10^{-9} mL $\cdot$ cell^{-1} $\cdot$ h^{-1}) and the detachment rate at the wall is fixed to a low value (10^{-1}h^{-1}), the parameter space for invasion is also wider in the two-compartment model than in the one-compartment model, and invasion is possible for all the parameter combinations (Fig. 6D).

3.4. Comparing pair-formation and bulk-conjugation models

Next, we compare plasmid invasion as predicted by the pair-formation and bulk-conjugation models. Surprisingly, the one-compartment pair-formation model results in the same parameter space where the plasmid can invade the plasmid-free equilibrium as the simpler one-compartment bulk-conjugation model that uses bulk-conjugation rates estimated from the output of the pair-formation models as described in Section 2.4 (Fig. A.4C). Furthermore, the two models predict the same dynamics over time (Fig. A.2). This is also true when the two-compartment pair-
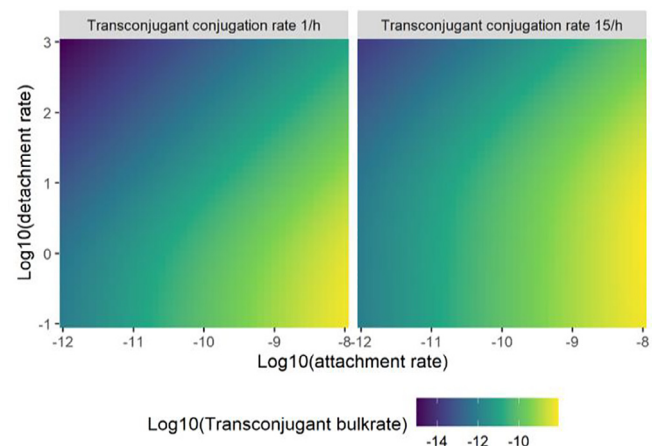

Fig. 7. Heatmaps showing the bulk-conjugation rates (mL $\cdot$ cell^{-1} $\cdot$ h^{-1}) of the transconjugant in the bulk-conjugation model for different intrinsic conjugation rates in the pair-formation model. Individual facets show increasing attachment rates from left to right and decreasing detachment rates from top to bottom.

formation model is compared with the two-compartment bulk-conjugation model (Fig. A.3). We could not generalize these results beyond our numerical simulations because we could not obtain an explicit analytic expression for the eigenvalues at the plasmid-free equilibrium of the pair-formation model. Analytic derivation shows the bulk-conjugation rate can be approximated by multiplying the intrinsic conjugation rate with the attachment rate divided by the detachment rate in the limit when the detachment rate goes to infinity (Section 5 of the Supplement). However, the assumption of a large detachment rate does not hold for our parameter space, and indeed the bulk-conjugation model using calculated bulk-conjugation rates does not result in the same parameter space where the plasmid can invade the plasmid-free equilibrium as the pair-formation model (right-hand side of Fig. A.4C).

As expected, the bulk-conjugation rates increase with increasing attachment rates and decreasing detachment rates (Fig. 7; Fig. A.1). High detachment rates lead to lower bulk-conjugation rates because most pairs detach before conjugation has occurred.

4. Discussion

We have extended a one-compartment pair-formation model describing plasmid dynamics to a two-compartment model with a liquid compartment representing the gut lumen and a surface-like compartment representing the gut wall. The additional compartment makes it possible to take differences in pair-formation kinetics between the two compartments into account. We also compared the pair-formation models with bulk-conjugation models to investigate if they lead to a different parameter space for invasion, or to other dynamics over time.

Our results show the additional compartment in two-compartment models enables invasion of plasmids for parameter values in the lumen for which invasion is not possible in the one-compartment model (Fig. 6). This occurs if migration to the wall prevents washout, leading to a higher density at the wall. This higher density, combined with mass-action dynamics for attachment and conjugation, then enables invasion of plasmids for low attachment rates in the lumen and at the wall, for which invasion is not possible in the one-compartment model (Fig. 6C, see also Fig. 5 showing the effect of differences in cell density caused by differences in rates of migration between the two compartments). If the attachment rate at the wall is high and the detachment rate at the wall is low, invasion is also possible in the two-compartment model for low attachment rates in the lumen for which invasion is not possible in the one-compartment model (Fig. 6D, see also Fig. 4). Higher bulk-conjugation rates on mucus from the mice gut than in gut contents in *in vitro* experiments (Licht et al., 1999) suggest this is relevant *in vivo*.

These extended possibilities for the plasmid to invade in the two-compartment model compared with the one-compartment model show the need to determine parameter values characterizing the wall compartment to describe plasmid dynamics in the gut. The importance of a wall compartment has previously been shown for in vitro systems that mimic the gut, where extension with a mucosal compartment led to invasion patterns that more closely resembled *in vivo* invasion patterns. Likely reasons for this are the persistence of wall-adhering strains that are washed out of the conventional lumen models (Freter et al., 1983b; Van den Abbeele et al., 2013), and species that inhabit the mucus but not the lumen (Van den Abbeele et al., 2012).

No experimental data on migration rates between the gut lumen and wall could be obtained from literature, so we used values from a previous modelling study (Imran et al., 2005). The cell density in the lumen could be derived from the literature (Table A.1), but the density at the gut wall was unknown as well.

Therefore, we choose to incorporate the biomass at the wall as additional biomass when extending the one-compartment model to a two-compartment model, instead of distributing the biomass in the one-compartment model between the lumen and the wall compartment. We have not attempted to scale densities to account for differences in the volumes of the compartments, because the ratio of these volumes is also not known. Moreover, the equilibrium cell densities likely differ between the compartments and vary across species. Given this uncertainty in parameter values, our results should be considered qualitatively rather than quantitatively, to guide the formulation of new hypotheses and the design of new experimental studies. To account for the uncertainty in parameter values, the densities and migration rates were varied across model simulations (Fig. 2; Fig. 5; Fig. 6).

The two compartments are modelled as homogenous well-mixed environments. In reality, chemical gradients along the length and width of the gut will result in gradients in growth rates and conjugation rates in the bacterial population, leading to heterogeneity within the two compartments (Slater et al., 2008; Stalder and Top, 2016). In addition, the fixed location at the wall impairs mixing of the bacteria, such that conjugation at the wall might cease after all donors have conjugated with their direct neighbours. This would lower the overall conjugation rate at the wall, and allow for the persistence of plasmid-free cells (Licht et al., 1999; Stalder and Top, 2016). Agent-based models could be used to take both types of heterogeneity into account (Krone et al., 2007; Zhong et al., 2012), and models using partial differential equations could be used to take the former type of heterogeneity into account (Grover and Wang, 2019; Imran et al., 2005).

Our results show that bulk-conjugation models accurately capture the description of plasmid dynamics given by pair-formation models, both in determining the stability of the plasmid-free equilibrium and in capturing the dynamics over time (Figs. A.2 – A.3). However, the more mechanistic description of conjugation in pair-formation models enables the incorporation of environmental conditions such as mechanic disruption (Zhong et al., 2010). This advantage comes at the expense of requiring more variables and parameters for the different pairs as additional populations. The currently implemented method to calculate bulk-conjugation rates (Equations (5) – (6); Equations A.2 – A.3; Fig. 7; Fig. A.1) has not been optimized for attachment rates higher than 10^{-8}. Since attachment rates higher than 10^{-8} mL · cell^{-1} · h^{-1} are improbable (Sheppard et al., 2020; Zhong et al., 2010), we decided to take 10^{-8} as an upper limit to the attachment rate.

Plasmid costs and the intrinsic conjugation rate of the donor do not limit invasion of the plasmid in our models, since the eigenvalues containing donor characteristics are always negative (see Section 6 of the supplement). Provided that the donor can conjugate (i.e., the conjugation and attachment rate of the donor are higher than zero), the donor will transfer the plasmid to recipients, giving rise to the transconjugant population. Subsequently, transconjugant characteristics will determine if the plasmid can invade. Earlier models of conjugation only distinguished plasmid-free from plasmid-bearing bacteria (Imran et al., 2005; Lopatkin et al., 2017; Simonsen, 1991; Stewart and Levin, 1977), or used identical parameter values for donors and transconjugants (Levin et al., 1979; Zhong et al., 2010). Intuitively this choice makes sense because most conjugation will occur between transconjugants and recipients if a rare donor invades, and here we show this is indeed appropriate if the plasmid-bearing bacteria are assigned the transconjugant characteristics. The reduction in the number of populations, and thus equations, if the donors and transconjugants are not considered as separate populations makes it easier to analyse the models, for example, as Imran *et al.* did for a two-compartment bulk-conjugation model (Imran et al., 2005). For the pair-formation models, this would

J.B. Alderliesten, M.P. Zwart, J. Arjan G.M. de Visser et al.

Journal of Theoretical Biology 533 (2022) 110937

result in only four populations per compartment: single recipients, single transconjugants, recipient-transconjugant pairs, and transconjugant-transconjugant pairs.

The importance of transconjugant characteristics to determine if plasmids can invade also implies the transfer of plasmids from non-host-adapted bacterial strains to host-adapted bacterial strains in an animal is important. As a consequence, risk assessment of plasmid-mediated antibiotic resistance based on the invasion of the donor strain might underestimate the actual potential for invasion. Although donor characteristics do not influence invasion in our models, donor characteristics are important when only few donors are present because of stochasticity in the survival of donors before plasmid transfer occurred. Extending the models to incorporate the influence of these stochastic processes would require the use of stochastic models such as presented in (Volkova et al., 2013). Furthermore, the presence of antibiotics and plasmids conferring resistance against those antibiotics (Baker et al., 2016) would increase the potential for invasion of plasmid-bearing donors due to positive selection.

5. Conclusions

Expanding one-compartment models of conjugation to two-compartment models by adding a wall compartment widens the range of parameter values for which plasmids can invade. Experimental data on migration rates between the gut lumen and the gut wall, and data on bacterial densities at the gut wall of relevant host species are needed to more accurately parameterize the models and to test the relevance of the parameter values explored in our study. Our findings show that bulk-conjugation models capture pair-formation dynamics well, and show that transconjugant characteristics rather than donor characteristics should be used to parameterize the models because donors are not limiting invasion.

Funding

CRediT authorship contribution statement

Jesse B. Alderliesten: Conceptualization, Methodology, Software, Formal analysis, Writing – original draft, Writing – review & editing, Visualization. **Mark P. Zwart:** Conceptualization, Writing – review & editing. **J. Arjan G.M. de Visser:** Conceptualization, Writing – review & editing. **Arjan Stegeman:** Conceptualization, Writing – review & editing, Funding acquisition. **Egil A.J. Fischer:** Conceptualization, Methodology, Writing – review & editing, Funding acquisition.

Declaration of Competing Interest

The authors declare that they have no known competing financial interests or personal relationships that could have appeared to influence the work reported in this paper.

Appendix A. Supplementary data

Supplementary data to this article can be found online at https://doi.org/10.1016/j.jtbi.2021.110937.

References

Alderliesten, J.B., Duxbury, S.J.N., Zwart, M.P., de Visser, J.A.G.M., Stegeman, A., Fischer, E.A.J., 2020. Effect of donor-recipient relatedness on the plasmid conjugation frequency: a meta-analysis. BMC Microbiol 20, 135. https://doi.org/10.1186/s12866-020-01825-4.

Baker, M., Hobman, J.L., Dodd, C.E.R, Ramsden, S.J., Stekel, D.J., Smalla, K., 2016. Mathematical modelling of antimicrobial resistance in agricultural waste highlights importance of gene transfer rate. FEMS Microbiol Ecol 92 (4), fiw040. https://doi.org/10.1093/femsec/fiw040.

Carroll, A.C., Wong, A., 2018. Plasmid persistence: costs, benefits, and the plasmid paradox. Can J Microbiol 64 (5), 293–304. https://doi.org/10.1139/cjm-2017-0609.

Dame-Korevaar, A., Fischer, E.A.J., van der Goot, J., Stegeman, A., Mevius, D., 2019. Transmission routes of ESBL/pAmpC producing bacteria in the broiler production pyramid, a literature review. Prev Vet Med 162, 136–150. https://doi.org/10.1016/j.prevetmed.2018.12.002.

Dib, J.R., Wagenknecht, M., Farías, M.E., Meinhardt, F., 2015. Strategies and approaches in plasmidome studies-uncovering plasmid diversity disregarding of linear elements? Front Microbiol 6, 463. https://doi.org/10.3389/fmicb.2015.00463.

Edelstein-Keshet, L., 2005. Mathematical models in biology. Society for industrial and applied mathematics, Philadelphia.

Freter, R., Freter, R.R., Brickner, H., 1983a. Experimental and mathematical models of Escherichia coli plasmid transfer in vitro and in vivo. Infect Immun 39 (1), 60–84. https://doi.org/10.1128/iai.39.1.60-84.1983.

Freter, R., Stauffer, E., Cleven, D., Holdeman, L.V., Moore, W.E., 1983b. Continuous-flow cultures as in vitro models of the ecology of large intestinal flora. Infect Immun 39 (2), 666–675. https://doi.org/10.1128/iai.39.2.666-675.1983.

Grover, J.P., Wang, F.B., 2019. Parasitic plasmid-host dynamics and host competition in flowing habitats. Math Biosci 311, 109–124. https://doi.org/10.1016/j.mbs.2019.03.001.

Imran, M., Jones, D., Smith, H., 2005. Biofilms and the plasmid maintenance question. Math Biosci 193 (2), 183–204. https://doi.org/10.1016/j.mbs.2004.10.008.

Krone, S.M., Lu, R., Fox, R., Suzuki, H., Top, E.M., 2007. Modelling the spatial dynamics of plasmid transfer and persistence. Microbiology 153, 2803–2816. https://doi.org/10.1099/mic.0.2006/004531-0.

Leclerc, Q.J., Lindsay, J.A., Knight, G.M., 2019. Mathematical modelling to study the horizontal transfer of antimicrobial resistance genes in bacteria: current state of the field and recommendations. J R Soc Interface 16 (157), 20190260. https://doi.org/10.1098/rsif.2019.0260.

Levin, B.R., Stewart, F.M., Rice, V.A., 1979. The kinetics of conjugative plasmid transmission: fit of a simple mass action model. Plasmid 2 (2), 247–260. https://doi.org/10.1016/0147-619X(79)90043-X.

Licht, T.R., Christensen, B.B., Krogfelt, K.A., Molin, S., 1999. Plasmid transfer in the animal intestine and other dynamic bacterial populations: the role of community structure and environment. Microbiology 145, 2615–2622. https://doi.org/10.1099/00221287-145-9-2615.

Lopatkin, A.J., Meredith, H.R., Srimani, J.K., Pfeiffer, C., Durrett, R., You, L., 2017. Persistence and reversal of plasmid-mediated antibiotic resistance. Nat Commun 8, 1689. https://doi.org/10.1038/s41467-017-01532-1.

McInnes, R.S., McCallum, G.E., Lamberte, L.E., van Schaik, W., 2020. Horizontal transfer of antibiotic resistance genes in the human gut microbiome. Curr Opin Microbiol 53, 35–43. https://doi.org/10.1016/j.mib.2020.02.002.

Mitchell, M.A., Lemme, A., 2008. Examination of the composition of the luminal fluid in the small intestine of broilers and absorption of amino acids under various ambient temperatures measured *in vivo*. Int J Poult Sci 7 (3), 223–233. https://doi.org/10.3923/ijps.2008.223.233.

R Core Team, 2020. R: A language and environment for statistical computing. R Foundation for Statistical Computing, Vienna, Austria. https://www.R-project.org/.

San Millan, A., MacLean, R.C., 2017. Fitness costs of plasmids: a limit to plasmid transmission. Microbiol Spectr 5 (5). https://doi.org/10.1128/microbiolspec.MTBP-0016-2017.

Savory, C.J., Mitchell, M.A., 1991. Absorption of hexose and pentose sugars in vivo in perfused intestinal segments in the fowl. Comp Biochem Physiol A Comp Physiol 100 (4), 969–974. https://doi.org/10.1016/0300-9629(91)90324-6.

Sheppard, R.J., Beddis, A.E., Barraclough, T.G., 2020. The role of hosts, plasmids and environment in determining plasmid transfer rates: a meta-analysis. Plasmid 108, 102489. https://doi.org/10.1016/j.plasmid.2020.102489.

Shintani, M., Sanchez, Z.K., Kimbara, K., 2015. Genomics of microbial plasmids: classification and identification based on replication and transfer systems and host taxonomy. Front Microbiol 6, 242. https://doi.org/10.3389/fmicb.2015.00242.

Shterzer, N., Mizrahi, I., 2015. The animal gut as a melting pot for horizontal gene transfer. Can J Microbiol 61 (9), 603–605. https://doi.org/10.1139/cjm-2015-0049.

Simonsen, L., 1991. The existence conditions for bacterial plasmids: theory and reality. Microb Ecol 22 (1), 187–205. https://doi.org/10.1007/BF02540223.

Slater, F.R., Bailey, M.J., Tett, A.J., Turner, S.L., 2008. Progress towards understanding the fate of plasmids in bacterial communities. FEMS Microbiology Ecology 66, 3–13. https://doi.org/10.1111/j.1574-6941.2008.00505.x.

J.B. Alderliesten, M.P. Zwart, J. Arjan G.M. de Visser et al.

Journal of Theoretical Biology 533 (2022) 110937

Smillie, C., Garcillán-Barcia, M.P., Francia, M.V., Rocha, E.P.C., de la Cruz, F., 2010. Mobility of plasmids. Microbiol Mol Biol Rev 74 (3), 434–452. https://doi.org/10.1128/MMBR.00020-10.

Soetaert, K., 2009. rootSolve: nonlinear root finding, equilibrium and steady-state analysis of ordinary differential equations.

Soetaert, K., Petzoldt, T., Setzer, R.W., 2010. Solving differential equations in R: package deSolve. J Stat Softw 33, 1–25. https://doi.org/10.18637/jss.v033.i09.

Stalder, T., Top, E., 2016. Plasmid transfer in biofilms: a perspective on limitations and opportunities. NPJ Biofilms Microbiomes 2, 16022. https://doi.org/10.1038/npjbiofilms.2016.22.

Stemmons, E.D., Smith, H.L., 2000. Competition in a chemostat with wall attachment. SIAM J Appl Math 61 (2), 567–595. https://doi.org/10.1137/S0036139999358131.

Stewart, F.M., Levin, B.R., 1977. The population biology of bacterial plasmids: a priori conditions for the existence of conjugationally transmitted factors. Genetics 87, 209–228. https://doi.org/10.1093/genetics/87.2.209.

Thomas, C.M., Nielsen, K.M., 2005. Mechanisms of, and barriers to, horizontal gene transfer between bacteria. Nat Rev Microbiol 3 (9), 711–721. https://doi.org/10.1038/nrmicro1234.

Van den Abbeele, P., Belzer, C., Goossens, M., Kleerebezem, M., De Vos, W.M., Thas, O., De Weirdt, R., Kerckhof, F.-M., Van de Wiele, T., 2013. Butyrate-producing Clostridium cluster XIVa species specifically colonize mucins in an in vitro gut model. ISME J. 7 (5), 949–961. https://doi.org/10.1038/ismej.2012.158.

Van den Abbeele, P., Roos, S., Eeckhaut, V., MacKenzie, D.A., Derde, M., Verstraete, W., Marzorati, M., Possemiers, S., Vanhoecke, B., Van Immerseel, F., Van de Wiele, 2012. Incorporating a mucosal environment in a dynamic gut model results in a more representative colonization by lactobacilli. Microb Biotechnol 5, 106–115. https://doi.org/10.1111/j.1751-7915.2011.00308.x.

Vogwill, T., MacLean, R.C., 2015. The genetic basis of the fitness costs of antimicrobial resistance: a meta-analysis approach. Evol Appl 8 (3), 284–295. https://doi.org/10.1111/eva.2015.8.issue-310.1111/eva.12202.

Volkova, V.V., Lu, Z., Lanzas, C., Scott, H.M., Grohn, Y.T., 2013. Modelling dynamics of plasmid-gene mediated antimicrobial resistance in enteric bacteria using stochastic differential equations. Sci Rep 3, 2463. https://doi.org/10.1038/srep02463.

Wickham, H., 2016. ggplot2: elegant graphics for data analysis. Springer-Verlag, New York.

Zhao, Y., Liu, D., Huang, W., Yang, Y., Ji, M., Nghiem, L.D., Trinh, Q.T., Tran, N.H., 2019. Insights into biofilm carriers for biological wastewater treatment processes: current state-of-the-art, challenges, and opportunities. Bioresour Technol 288, 121619. https://doi.org/10.1016/j.biortech.2019.121619.

Zhong, X., Krol,, J.E., Top, E.M., Krone, S.M., 2010. Accounting for mating pair formation in plasmid population dynamics. J Theor Biol 262 (4), 711–719. https://doi.org/10.1016/j.jtbi.2009.10.013.

Zhong, X., Droesch, J., Fox, R., Top, E.M., Krone, S.M., 2012. On the meaning and estimation of plasmid transfer rates for surface-associated and well-mixed bacterial populations. J Theor Biol 294, 144–152. https://doi.org/10.1016/j.jtbi.2011.10.034.